



Layer photovoltaic effect in van der Waals heterostructures

Oles Matsyshyn , Ying Xiong, Arpit Arora , and Justin C. W. Song*
 Division of Physics and Applied Physics, School of Physical and Mathematical Sciences,
 Nanyang Technological University, Singapore 637371



(Received 30 January 2023; accepted 26 April 2023; published 16 May 2023)

We argue that the layer electric polarization of noncentrosymmetric layered heterostructures can be generically controlled by light yielding a layer photovoltaic effect (LPE). The LPE possesses a rich phenomenology and can arise from myriad distinct mechanisms displaying strong sensitivity to symmetry (e.g., point group and time reversal) as well as the presence/absence of a Fermi surface. We systematically classify these and unveil how LPE manifests for a range of light polarizations. Strikingly, LPE manifests even for unpolarized light in rotationally symmetric heterostructures, sharply contrasting with that of in-plane photocurrent responses. These unusual layer photoresponses can be realized in a range of layered heterostructures such as bilayer graphene aligned on hexagonal boron nitride and manifest sizable layer polarization susceptibilities in the terahertz frequency range that can be used as a means of bulk photodetection.

DOI: [10.1103/PhysRevB.107.205306](https://doi.org/10.1103/PhysRevB.107.205306)

I. INTRODUCTION

Mechanical stacks of atomically thin van der Waals (vdW) materials enable building quantum phases from the bottom up with properties that go beyond that of its individual constituent components [1,2]. A particularly striking example is the emergence of a layer degree of freedom in stacks. Manipulating the relative degree with which each of the layers is charged, as characterized by its static interlayer polarization, affords the means to dramatically engineer band structures [3,4], tune quantum geometric properties [5–8], as well as realize correlated phases of matter [9–12]. Since interlayer polarization points out of plane, it is highly sensitive to vertical displacement fields. As a result, it has been traditionally controlled by toggling voltages sustained across a dual top and bottom gate sandwich architecture [3].

Here, we argue that interlayer polarization in noncentrosymmetric layered heterostructures can be generically controlled by light manifesting a *layer photovoltaic effect* (LPE). Such LPE responses appear to be second order in the incident light electromagnetic (EM) field, and, as we show below, come in myriad distinct types; by performing a systematic classification we delineate LPEs with distinct symmetry constraints, light polarization dependence, as well as physical origins. Importantly, we find LPEs can arise from both resonant interband absorption as well as off-resonant virtual processes in either metallic or insulating states, providing a versatile means to control interlayer polarization across different phases of matter.

Strikingly, LPE is generically present even if in-plane charge photocurrent vanishes. An example of such an LPE was recently predicted in twisted bilayer graphene where

the interband absorption of circularly polarized light in handed stacks induces a helicity-dependent photoinduced interlayer polarization [13] even as C_2 symmetry zeros in-plane photocurrents. Our work predicts a wide range of LPE responses beyond those known previously: For instance, we find LPE can manifest even in rotationally symmetric vdW heterostructures under *unpolarized* light. This sharply contrasts to conventional bulk in-plane photocurrent responses for unpolarized light that vanish in rotationally symmetric vdW materials [14]. In particular, at high frequencies corresponding to interband transitions we find an injectionlike process enables *unpolarized* (nonhelical) light to induce a (second-order) nonlinear LPE even in an *achiral* and noncentrosymmetric vdW layered heterostructure (see Fig. 1).

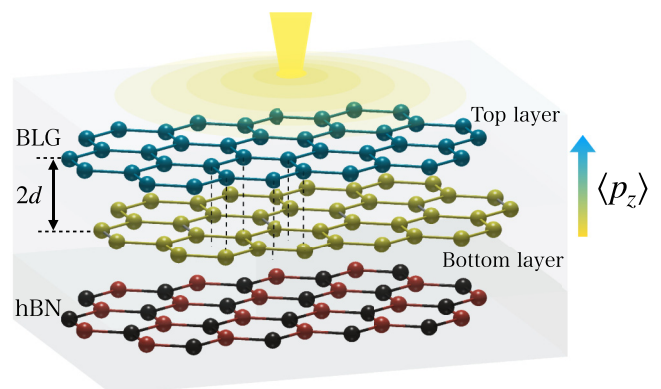


FIG. 1. Layer photovoltaic effect and interlayer polarization. Photoinduced nonlinear interlayer polarization (here denoted by $\langle p_z \rangle$) in noncentrosymmetric van der Waals stacks; we term this the layer photovoltaic effect (LPE). Here, an example of a noncentrosymmetric and achiral vdW structure is shown: bilayer graphene aligned with hexagonal boron nitride (BLG/hBN). These achiral structures possess LPE induced by nonhelical light.

*Corresponding author: justinsong@ntu.edu.sg

Surprisingly, the injectionlike process also produces an interlayer current even as the electrons do not possess an out-of-plane velocity. Instead, this intrinsic interlayer current arises from the pumping of the interlayer polarization. Additionally, even at low frequency without interband transitions, we find different types of large LPE responses that can be induced in the metallic regime. As we will see, these metallic contributions arise from the momentum-space asymmetry in the layer polarization of Bloch states on the Fermi surface.

We anticipate that the LPEs we unveil can be used in bulk photodetection schemes that do not require p - n junctions. Since many noncentrosymmetric vdW stacks are achiral possessing mirror symmetries that render helicity-dependent LPE vanishing, nonhelical LPEs are crucial in activating interlayer polarization responses. Indeed, as we discuss below, the injection and metallic LPEs we unveil in our work can achieve giant susceptibility values in bilayer graphene (BLG) aligned with hexagonal boron nitride (hBN) heterostructures, orders of magnitude larger than those reported in chiral stacks [13] and manifesting even for unpolarized light.

II. INTERLAYER POLARIZATION RESPONSE

We begin by directly examining the LPE response which is directly connected to the layer degree of freedom l . The interlayer polarization operator is

$$\hat{P}^z = ed \sum_{\alpha_l} \hat{l} |\alpha_l\rangle \langle \alpha_l| = \hat{p}^z d, \quad (1)$$

where \hat{l} is the layer index operator, $\hat{l} |\alpha_l\rangle = l |\alpha_l\rangle$, and $|\alpha_l\rangle$ are orbitals localized on layer l . For clarity, here we concentrate on a bilayer system with an interlayer distance $2d$ (see Fig. 1). Our theory, however, is general and can be readily applied to multilayered systems.

When light is normally incident on the vdW stack (see Fig. 1), an out-of-plane static interlayer polarization can be induced. To see this, first consider the Hamiltonian $\hat{H}(\mathbf{k}, t) = H_0(\mathbf{k}) + H_E(\mathbf{k}, t)$, where $H_0(\mathbf{k})$ is the bare Hamiltonian with $|u_{n\mathbf{k}}\rangle$ and $\epsilon_n(\mathbf{k})$ the corresponding Bloch states and eigenenergies; here and below, roman indices denote band indices. $H_E(\mathbf{k}, t)$ describes the light-matter interaction. For a monochromatic EM field, $H_E(\mathbf{k}, t) = e\hat{\mathbf{r}} \cdot [\mathbf{E}e^{i\Omega t} + \mathbf{E}^*e^{-i\Omega t}]e^{\eta t}$ [15,16], with $\hat{\mathbf{r}}$ the position operator, $\eta \rightarrow 0^+$ an adiabatic turn-on parameter, and Ω is the frequency of the light.

The LPE can be obtained from Eq. (1) as $\langle P^z(t) \rangle = \int \text{Tr}[\hat{\rho}(t)\hat{P}^z]d\mathbf{k}/(2\pi)^2$, where $\hat{\rho}$ is the density matrix. Here, the evolution of the density matrix and the resulting photoinduced interlayer polarization can be tracked in a standard perturbative fashion (see Supplemental Material [17]). This produces a second-order nonlinear photoinduced static interlayer polarization $\langle \delta P_{\text{st}}^z \rangle$ characterized by an LPE susceptibility tensor $\chi(\omega)$ as

$$\langle \delta P_{\text{st}}^z \rangle = 2d \sum_{\alpha\beta} \text{Re}[E^\alpha E^{\beta*} \chi^{\alpha\beta}(\Omega)], \quad (2)$$

where α, β are spatial indices (x or y). We will show there are five contributions to $\chi^{\alpha\beta}(\omega)$ with distinct physical origins, symmetry properties, and phenomenology.

To proceed, it is useful to delineate between interband and intraband responses and for concreteness we will confine ourselves to band nondegenerate systems. Three contributions comprise interband responses, injection (I), shift (S), and Fermi sea (FS),

$$\chi_{\text{inter}}^{\alpha\beta}(\omega) = \chi_{\text{I}}^{\alpha\beta}(\omega) + \chi_{\text{S}}^{\alpha\beta}(\omega) + \chi_{\text{FS}}^{\alpha\beta}(\omega), \quad (3)$$

where χ_{I} and χ_{S} describe LPE arising from resonant real interband excitations, whereas χ_{FS} is off resonant.

The injection susceptibility is $\chi_{\text{I}}^{\alpha\beta}(\omega) = \tau \sigma_{\text{inter}}^{\alpha\beta}(\omega)/4$ with

$$\sigma_{\text{inter}}^{\alpha\beta}(\omega) = \frac{\pi e^2}{\hbar^2} \sum_{n,m,\mathbf{k}} \delta(\omega + \omega_{nm}) A_{nm}^\alpha A_{mn}^\beta f_{nm} \delta P_{mn}, \quad (4)$$

where $f_{nm} = f[\epsilon_n(\mathbf{k})] - f[\epsilon_m(\mathbf{k})]$ is the difference between Fermi functions in different bands, $\hbar\omega_{nm} = \epsilon_n(\mathbf{k}) - \epsilon_m(\mathbf{k})$, and $\delta P_{mn} = p_{mm}^z - p_{nn}^z$ is the difference between layer polarization between the final and initial states. $p_{nm}^z = \langle u_{n\mathbf{k}} | \hat{p}^z | u_{m\mathbf{k}} \rangle$ is a matrix element of the polarization operator and $A_{nm}^\alpha = i \langle u_{n\mathbf{k}} | \partial_{\mathbf{k}_\alpha} | u_{m\mathbf{k}} \rangle$ is the interband Berry connection [18]. Here, τ is a phenomenological relaxation time [19] that regularizes the χ_{I} response.

$\chi_{\text{I}}(\omega)$ represents the first result of our work and arises from the contrasting interlayer polarization when an electron transitions from state $n, \mathbf{k} \rightarrow m, \mathbf{k}$: Its polarization changes from $p_{nn} \rightarrow p_{mm}$. As we will argue below, this process also yields an anomalous photoinduced interlayer current, controlled by an interlayer conductivity $\sigma_{\text{inter}}^{\alpha\beta}(\omega)$. This anomalous interlayer current acts as a source that pumps the interlayer electric polarization. As a result, $\chi_{\text{I}}(\omega)$ grows with τ yielding large LPE. This picture is similar to how bulk injection photocurrents are often understood as arising from a photoinduced acceleration [19,20].

Injection LPE contrasts with that of the shift LPE, $\chi_{\text{S}}(\omega)$, recently discussed in Ref. [13],

$$\chi_{\text{S}}^{\alpha\beta}(\omega) = \pi \frac{e^2}{\hbar^2} \sum_{n,m,\mathbf{k}} \delta(\omega + \omega_{nm}) f_{nm} A_{nm}^\alpha \mathcal{M}_{mn}^\beta, \quad (5)$$

where

$$\mathcal{M}_{mn}^\beta = \partial^\beta \frac{p_{mn}}{\omega_{mn}} - i \sum_c \left[A_{mc}^\beta \frac{\bar{p}_{cn}^z}{\omega_{cn}} - \frac{\bar{p}_{mc}^z}{\omega_{mc}} A_{cn}^\beta \right], \quad (6)$$

and $\bar{p}_{nm}^z = p_{nm}^z(1 - \delta_{nm})$. χ_{S} is intrinsic (τ independent) and arises from an interlayer coordinate shift that is nonvanishing in chiral media.

In contrast to the other interband responses, $\chi_{\text{FS}}(\omega)$ does not require real transitions. Instead, it corresponds to nonlinear interlayer polarization sustained even for light with frequency below the band gap of an insulator. It is written as $\chi_{\text{FS}}^{\alpha\beta}(\omega) = \chi_{\text{FS},1}^{\alpha\beta}(\omega) + \chi_{\text{FS},2}^{\alpha\beta}(\omega)$, where

$$\chi_{\text{FS},1}^{\alpha\beta}(\omega) = \frac{e^2}{2\hbar^2} \sum_{n,m,\mathbf{k}} A_{nm}^\alpha A_{mn}^\beta f_{nm} \mathcal{P} \left[\frac{p_{mn}^z - p_{nn}^z}{(\omega + \omega_{nm})^2} \right], \quad (7)$$

$$\chi_{\text{FS},2}^{\alpha\beta}(\omega) = i \frac{e^2}{\hbar^2} \sum_{n,m,\mathbf{k}} f_{nm} A_{nm}^\alpha \mathcal{M}_{mn}^\beta \mathcal{P} \left[\frac{1}{\omega + \omega_{nm}} \right], \quad (8)$$

where \mathcal{P} denotes the principal part. Strikingly, this off-resonant LPE survives even for insulators (unlike its photocurrent counterpart [21,22]). As a result, we denote it a Fermi-sea LPE since it arises from virtual processes between completely occupied and unoccupied bands. χ_{FS} proceeds in much the same fashion as that of the conventional dielectric response in insulators where similar virtual processes contribute to dynamical screening. Indeed, χ_{FS} can be understood as its nonlinear rectified counterpart.

The last LPEs we unveil are intraband in nature: These depend on the presence of a Fermi surface and exhibit a low-frequency divergence characteristic of metallic responses in the clean limit. These are the semiclassical (SC) and Berry (B) LPE responses, $\chi_{\text{intra}}(\omega) = \chi_{\text{SC}}(\omega) + \chi_{\text{B}}(\omega)$, with SC susceptibility,

$$\chi_{\text{SC}}^{\alpha\beta}(\omega) = \frac{e^2}{2\hbar^2} \sum_{n,\mathbf{k}} \frac{\partial^\alpha \partial^\beta f_n}{\omega^2 + \tau^{-2}} p_{nm}^z, \quad (9)$$

and Berry susceptibility,

$$\chi_{\text{B}}^{\alpha\beta}(\omega) = \frac{e^2}{\hbar^2} \sum_{n,m,\mathbf{k}} \frac{p_{nm}^z A_{mn}^{\alpha} i \partial^\beta f_{nm}}{(\omega + i\tau^{-1})\omega_{nm}}, \quad (10)$$

where intraband responses are regularized with a relaxation time τ [23]. Note that χ_{B} shares a similar density matrix origin to its counterpart in the more familiar but distinctly different photocurrent response (the Berry curvature dipole-induced nonlinear Hall effect [24]).

$\chi_{\text{SC}}(\omega)$ has a semiclassical origin: It arises from a dc shift (in momentum space) of the metallic Fermi surface induced by periodic driving; this enables picking out a dipolar distribution of $p_{nm}(\mathbf{k})$ in momentum space. $\chi_{\text{B}}(\omega)$ arises from interband coherences sustained from the periodic driving; unlike the other responses we have discussed, $\chi_{\text{B}}(\omega)$ has an odd parity under time reversal (cf. $\partial^\beta f$ term), vanishing in nonmagnetic materials. In what follows, we will focus on LPEs in time-reversal symmetry (TRS) preserving systems.

III. INTRINSIC OUT-OF-PLANE INTERLAYER CURRENT

We now proceed to argue that the origin of the large injection LPE arises from an anomalous *out-of-plane* interlayer current induced by oscillating *in-plane* electric fields. To see this, we note that the interlayer electric current is naturally described by $\hat{j}^z = d\hat{P}_z/dt = [\hat{P}_z, \hat{H}]/(i\hbar)$ [25]. Computing the expectation value of the interlayer current $\langle j^z(t) \rangle$, we find

$$\text{Tr}[\hat{j}^z \rho(t)] = \frac{1}{i\hbar} \text{Tr}\{[\hat{P}_z, \hat{H}]\rho(t)\} = \text{Tr}[P^z \dot{\rho}(t)], \quad (11)$$

where we have noted the cyclic property of the trace $\text{Tr}\{[A, B]C\} = \text{Tr}\{A[B, C]\}$ as well as employed the Liouville equation $i\hbar d\hat{\rho}(t)/dt = [\hat{H}(\mathbf{k}, t), \hat{\rho}(t)]$. In order to isolate the rectified interlayer current, we focus on the period average $j_{\text{rectified}}^z = [\int_0^T dt \lim_{\eta \rightarrow 0} \langle j^z(t) \rangle]/T$, where $T = 2\pi/\Omega$ is the period of the drive EM field. For a finite drive frequency Ω , this directly produces an out-of-plane interlayer current,

$$j_{\text{rectified}}^z = 2d \text{Re}[E^\alpha E^{\beta*} \sigma_{\text{inter}}^{\alpha\beta}(\Omega)], \quad (12)$$

that is driven by an oscillating in-plane electric field \mathbf{E} . Here, $\sigma_{\text{inter}}^{\alpha\beta}(\Omega)$ is the interlayer nonlinear conductivity found in

TABLE I. LPE mechanisms in TRS preserving systems. \uparrow indicates nonhelical mechanisms (induced by linearly polarized light), while \mathbf{C} indicates helical responses (induced by circularly polarized light). \checkmark denotes allowed, and \times indicates forbidden. SC and FS are semiclassical and Fermi sea, respectively. Note that χ_{B} (see text) is forbidden when TRS is preserved, but becomes activated when TRS is broken.

	SC	FS	Shift	Injection	Reported in
\uparrow	\checkmark	\checkmark	\times	\checkmark	This work
\mathbf{C}	\times	\times	\checkmark	\times	Ref. [13]

Eq. (4). Interestingly, Eq. (4) depends only on intrinsic band geometric quantities (e.g., A_{nm}^α , δP_{mn}).

We note that second-order nonlinear photocurrent susceptibilities have recently been the subject of intense investigation [15,16,23,26–37]. These have concentrated on photocurrents formed from bulk itinerant electrons with a well-defined velocity. In contrast, $\sigma_{\text{inter}}^{\alpha\beta}(\Omega)$ describes out-of-plane current in a vdW stack hosting electrons that do not have a z -direction velocity. Instead, the interlayer current can be understood as a type of electric polarization pump that injects polarization.

IV. SYMMETRY PROPERTIES OF LPE

The mechanisms for LPE discussed above have distinct symmetry properties. To see this, we rewrite Eq. (2) as

$$\begin{aligned} \frac{\langle \delta P_{\text{st}}^z \rangle}{d} &= \underbrace{(E^\alpha E^{*\beta} + E^{*\alpha} E^\beta)}_{\text{Linearly polarized light}} \underbrace{\frac{1}{2} [\chi^{\alpha\beta}(\Omega) + \chi^{\alpha\beta}(-\Omega)]}_{\text{Re}} \\ &+ \underbrace{(iE^\alpha E^{*\beta} - iE^{*\alpha} E^\beta)}_{\text{Circularly polarized light}} \underbrace{\frac{1}{2i} [\chi^{\alpha\beta}(\Omega) - \chi^{\alpha\beta}(-\Omega)]}_{\text{Im}}, \end{aligned} \quad (13)$$

displaying how the real (imaginary) parts of the susceptibility tensor control the response to linearly polarized (circularly polarized) irradiation. Recalling that under time-reversal symmetry we have $\mathbf{A}_{nm}(\mathbf{k}) = \mathbf{A}_{mn}(-\mathbf{k})$ and $p_{nm}(\mathbf{k}) = p_{mn}(-\mathbf{k})$, we obtain the nonhelical (linear) versus helical (circular) classification in Table I, namely χ_{I} , χ_{FS} , and χ_{SC} mediate responses to linearly polarized light but are helicity insensitive; χ_{S} , in contrast, only arises under circularly polarized irradiation. Naturally, inversion symmetry zeros out all LPE responses; see Supplemental Material [17] for details.

Point-group symmetries also play a critical role in constraining the LPE. For instance, in-plane mirror symmetry \mathcal{M}_y forces the off-diagonal components of the nonlinear LPE susceptibility tensor to vanish: $\chi^{xy}(\omega) = \chi^{yx}(\omega) = 0$. This disables helicity-dependent LPE. As a result, achiral vdW stacks (i.e., ones with a mirror plane) do not possess a helicity-dependent LPE. As a result, comparing with Table I, in these systems we find that LPE proceed from χ_{I} , χ_{FS} , and χ_{SC} only; χ_{S} vanishes.

In contrast, in chiral stacks that possess high crystalline symmetries, the opposite can be true. The combination of C_{n_z} ($n \geq 3$) and C_{2_x} point-group rotational symmetries can

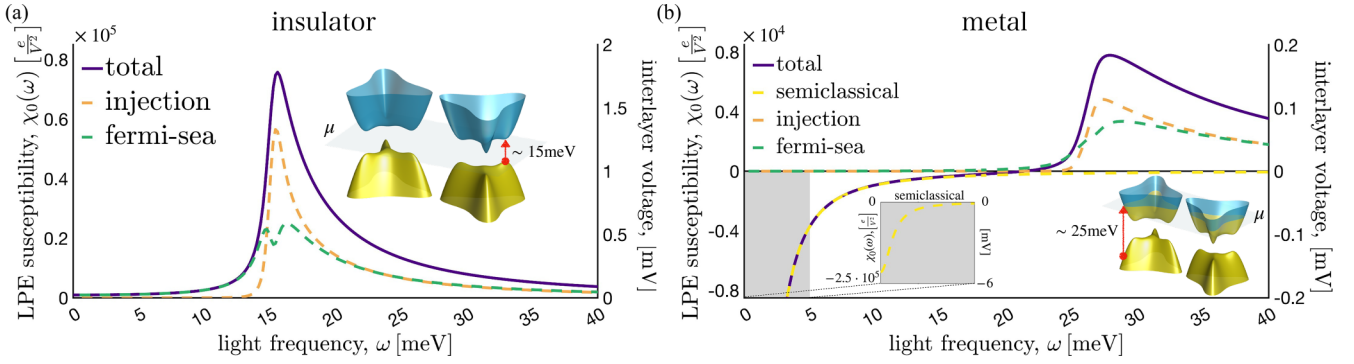


FIG. 2. Nonhelical LPE responses in vdW heterostructure. BLG/hBN LPE susceptibility tensor $\chi(\omega) = \chi_0(\omega)\mathbb{I}$ (left y axis) and the corresponding interlayer voltage difference (right y axis) photoinduced (for an intensity of 1 kW cm^{-2}) in the (a) insulating state ($\mu = 10 \text{ meV}$ in the gap) and (b) metallic state ($\mu = 20 \text{ meV}$) numerically evaluated using the low-energy Hamiltonian in Eq. (14). All quantities shown in the figure are per spin. Both χ_I (orange) and χ_{FS} (green) contribute to the total response (purple) in the insulating state. In the metallic state, an additional metallic χ_{SC} (yellow) emerges that dominates at low frequencies. The right insets in both panels display the low-energy band structure of BLG/hBN; μ indicates the Fermi level. The left inset in (b) shows a zoom-in of the gray region. Parameters used: $\tau = 1 \text{ ps}$ and $\Delta = 30 \text{ meV}$.

render nonhelical LPEs vanishing (see Ref. [13] for an explicit example in twisted bilayer graphene as well as a full symmetry analysis in Supplemental Material [17]). Of course, in chiral vdW stacks where at least one of these point-group rotational symmetries are broken, both helicity-dependent and nonhelical LPEs are allowed.

V. NONHELICAL LPE RESPONSE IN BLG/hBN

To exemplify the nonhelical LPE response from χ_I , χ_{FS} , and χ_{SC} in TRS preserving systems, we focus on an achiral vdW system: bilayer graphene aligned with hexagonal boron nitride (BLG/hBN). Aligned BLG/hBN breaks inversion symmetry, and possesses C_{3z} and \mathcal{M}_y symmetries while breaking C_{2x} (see Fig. 1). As a result, only nonhelical LPE responses are allowed; χ_S vanishes. Indeed, the presence of both C_{3z} and \mathcal{M}_y guarantees $\chi(\omega) = \chi_0(\omega)\mathbb{I}$, allowing LPE to manifest for unpolarized light.

We model the long-wavelength electronic excitations of BLG/hBN using a minimal low-energy Hamiltonian

$$\hat{H} = \begin{pmatrix} \Delta/2 & v\pi^\dagger & 0 & v_3\pi \\ v\pi & -\Delta/2 & \gamma_1 & 0 \\ 0 & \gamma_1 & 0 & v\pi^\dagger \\ v_3\pi^\dagger & 0 & v\pi & 0 \end{pmatrix}, \quad (14)$$

where $v = 0.639 \text{ eV nm}$ is the Dirac velocity of graphene, $v_3 = 0.081 \text{ eV nm}$ characterizes trigonal warping, $\gamma_1 = 0.4 \text{ eV}$ is the interlayer hopping, and $\pi = \xi k_x + ik_y$, where $\xi = \pm 1$ is the valley index. Using Eq. (1) the polarization operator reads as $\hat{p}_z = \text{diag}(1, 1, -1, -1)$. Responses of different valleys are added. Δ is the AB sublattice asymmetry induced by aligning one side with hBN, thereby breaking inversion symmetry and opening a gap in the spectrum (see the inset in Fig. 2). In what follows we will concentrate on low frequencies up to the terahertz range where large LPEs manifest. This is smaller than the energy range (150–200 meV) where superlattice effects from the hBN alignment ensue [38].

The LPE in BLG/hBN was numerically evaluated using Eqs. (4) and (7)–(9) at low temperature and summed across

both valleys for the electronic states in Eq. (14); LPE susceptibilities are plotted in Fig. 2; see Supplemental Material [17] for a full discussion of the numerical details. We find interband LPEs peak for frequencies close to the gap size; see Fig. 2(a) where χ_I and χ_{FS} are plotted when the chemical potential is in the gap. This indicates that both χ_I (orange) and χ_{FS} (green) are dominated by interband processes close to the band edge.

Interestingly, when the chemical potential is moved into the conduction band [Fig. 2(b)], a new metallic peak in the nonlinear LPE response emerges at low frequencies that corresponds to χ_{SC} (yellow); the interband LPE responses still persist but now appear at higher frequencies due to Pauli blocking (see the right inset). The metallic peak is particularly striking since it displays large responses (left inset) even for frequencies below any interband optical transition, as well as the opposite sign of susceptibilities as compared to the interband contributions.

The LPE we unveil demonstrates how stacking can introduce classes of responses not found in a single layer. Indeed, we anticipate that χ_I and χ_{SC} can produce large LPE several orders of magnitude larger than that previously known, e.g., in Ref. [13]. For instance, close to the interband peak in BLG/hBN heterostructures, we find a large interlayer surface charge density difference of order 20 nC cm^{-2} (this corresponds to an interlayer voltage of order 4 mV) can be sustained even for modest light intensities of 1 kW cm^{-2} . Here, we have accounted for spin degeneracy. At very low frequencies, LPE is expected to be even more pronounced, yielding interlayer voltages of the order of 10 mV under the same light intensity [see Fig. 2(b), left inset]. Such interlayer voltages can be readily detected using capacitive probes [39,40] or scanning electron transistors [41], and are not just confined to BLG/hBN (that we have focused on for a concrete illustration). Indeed, we expect that LPEs are generic and will manifest in the wide zoo of noncentrosymmetric layered heterostructures available, e.g., layered transition metal dichalcogenides. In addition to providing different means of photodetection (especially

in the THz regime), given the large LPE susceptibilities, the photoinduced interlayer polarizations may even enable light-driven means of switching the electric polarization in a range of vdW layered ferroelectrics that have recently become available [42–44].

ACKNOWLEDGMENTS

This work was supported by the Ministry of Education Singapore under its MOE AcRF Tier 3 Grant No. MOE 2018-T3-1-002 and a Nanyang Technological University start-up grant (NTU-SUG).

- [1] L. Balents, C. R. Dean, D. K. Efetov, and A. F. Young, *Nat. Phys.* **16**, 725 (2020).
- [2] J. C. Song and N. M. Gabor, *Nat. Nanotechnol.* **13**, 986 (2018).
- [3] Y. Zhang, T.-T. Tang, C. Girit, Z. Hao, M. C. Martin, A. Zettl, M. F. Crommie, Y. R. Shen, and F. Wang, *Nature (London)* **459**, 820 (2009).
- [4] Q. Tong, H. Yu, Q. Zhu, Y. Wang, X. Xu, and W. Yao, *Nat. Phys.* **13**, 356 (2017).
- [5] W. Yao, D. Xiao, and Q. Niu, *Phys. Rev. B* **77**, 235406 (2008).
- [6] J. C. Song and M. A. Kats, *Nano Lett.* **16**, 7346 (2016).
- [7] J. Yin, C. Tan, D. Barcons-Ruiz, I. Torre, K. Watanabe, T. Taniguchi, J. C. Song, J. Hone, and F. H. Koppens, *Science* **375**, 1398 (2022).
- [8] C. Ma, S. Yuan, P. Cheung, K. Watanabe, T. Taniguchi, F. Zhang, and F. Xia, *Nature (London)* **604**, 266 (2022).
- [9] G. Chen, L. Jiang, S. Wu, B. Lyu, H. Li, B. L. Chittari, K. Watanabe, T. Taniguchi, Z. Shi, J. Jung *et al.*, *Nat. Phys.* **15**, 237 (2019).
- [10] H. Zhou, T. Xie, A. Ghazaryan, T. Holder, J. R. Ehrets, E. M. Spanton, T. Taniguchi, K. Watanabe, E. Berg, M. Serbyn *et al.*, *Nature (London)* **598**, 429 (2021).
- [11] H. Zhou, T. Xie, T. Taniguchi, K. Watanabe, and A. F. Young, *Nature (London)* **598**, 434 (2021).
- [12] S. C. de la Barrera, S. Aronson, Z. Zheng, K. Watanabe, T. Taniguchi, Q. Ma, P. Jarillo-Herrero, and R. Ashoori, *Nat. Phys.* **18**, 771 (2022).
- [13] Y. Gao, Y. Zhang, and D. Xiao, *Phys. Rev. Lett.* **124**, 077401 (2020).
- [14] T. Akamatsu, T. Ideue, L. Zhou, Y. Dong, S. Kitamura, M. Yoshii, D. Yang, M. Onga, Y. Nakagawa, K. Watanabe *et al.*, *Science* **372**, 68 (2021).
- [15] C. Aversa and J. E. Sipe, *Phys. Rev. B* **52**, 14636 (1995).
- [16] J. E. Sipe and A. I. Shkrebtii, *Phys. Rev. B* **61**, 5337 (2000).
- [17] See Supplemental Material at <http://link.aps.org/supplemental/10.1103/PhysRevB.107.205306> for further theoretical details of the second-order response, discussion of symmetries, as well as description of numerics.
- [18] E. I. Blount, in *Solid State Physics*, edited by F. Seitz and D. Turnbull (Academic Press, New York, 1962), Vol. 13, pp. 305–73.
- [19] J. Ahn, G.-Y. Guo, and N. Nagaosa, *Phys. Rev. X* **10**, 041041 (2020).
- [20] F. de Juan, A. G. Grushin, T. Morimoto, and J. E. Moore, *Nat. Commun.* **8**, 15995 (2017).
- [21] L. Gao, Z. Addison, E. J. Mele, and A. M. Rappe, *Phys. Rev. Res.* **3**, L042032 (2021).
- [22] H. Watanabe and Y. Yanase, *Phys. Rev. X* **11**, 011001 (2021).
- [23] O. Matsyshyn and I. Sodemann, *Phys. Rev. Lett.* **123**, 246602 (2019).
- [24] I. Sodemann and L. Fu, *Phys. Rev. Lett.* **115**, 216806 (2015).
- [25] R. Resta and D. Vanderbilt, *Theory of Polarization: A Modern Approach* (Springer, Berlin, 2007), pp. 31–68.
- [26] L.-k. Shi, O. Matsyshyn, J. C. W. Song, and I. S. Villadiego, *Phys. Rev. B* **107**, 125151 (2023).
- [27] O. Matsyshyn, J. C. W. Song, I. Sodemann Villadiego, and L.-k. Shi, [arXiv:2301.00811](https://arxiv.org/abs/2301.00811) [cond-mat.mes-hall].
- [28] R. von Baltz and W. Kraut, *Phys. Rev. B* **23**, 5590 (1981).
- [29] W. Kraut and R. von Baltz, *Phys. Rev. B* **19**, 1548 (1979).
- [30] B. I. Sturman and V. M. Fridkin, *The Photovoltaic and Photorefractive Effects in Noncentrosymmetric Materials*, Ferroelectricity and Related Phenomena Vol. 8 (Gordon and Breach, Philadelphia, 1992).
- [31] J. A. Brehm, S. M. Young, F. Zheng, and A. M. Rappe, *J. Chem. Phys.* **141**, 204704 (2014).
- [32] T. Morimoto and N. Nagaosa, *Sci. Adv.* **2**, e1501524 (2016).
- [33] N. Nagaosa and T. Morimoto, *Adv. Mater.* **29**, 1603345 (2017).
- [34] D. E. Parker, T. Morimoto, J. Orenstein, and J. E. Moore, *Phys. Rev. B* **99**, 045121 (2019).
- [35] O. Matsyshyn, F. Piazza, R. Moessner, and I. Sodemann, *Phys. Rev. Lett.* **127**, 126604 (2021).
- [36] O. Matsyshyn, U. Dey, I. Sodemann, and Y. Sun, *J. Phys. D* **54**, 404001 (2021).
- [37] Q. Ma, R. Krishna Kumar, S.-Y. Xu, F. H. L. Koppens, and J. C. W. Song, *Nat. Rev. Phys.* **5**, 170 (2023).
- [38] M. Yankowitz, J. Xue, D. Cormode, J. D. Sanchez-Yamagishi, K. Watanabe, T. Taniguchi, P. Jarillo-Herrero, P. Jacquod, and B. J. LeRoy, *Nat. Phys.* **8**, 382 (2012).
- [39] A. F. Young and L. S. Levitov, *Phys. Rev. B* **84**, 085441 (2011).
- [40] A. F. Young, C. R. Dean, I. Meric, S. Sorgenfrei, H. Ren, K. Watanabe, T. Taniguchi, J. Hone, K. L. Shepard, and P. Kim, *Phys. Rev. B* **85**, 235458 (2012).
- [41] J. Martin, B. E. Feldman, R. T. Weitz, M. T. Allen, and A. Yacoby, *Phys. Rev. Lett.* **105**, 256806 (2010).
- [42] Z. Zheng, Q. Ma, Z. Bi, S. de la Barrera, M.-H. Liu, N. Mao, Y. Zhang, N. Kiper, K. Watanabe, T. Taniguchi *et al.*, *Nature (London)* **588**, 71 (2020).
- [43] X. Wang, K. Yasuda, Y. Zhang, S. Liu, K. Watanabe, T. Taniguchi, J. Hone, L. Fu, and P. Jarillo-Herrero, *Nat. Nanotechnol.* **17**, 367 (2022).
- [44] K. Yasuda, X. Wang, K. Watanabe, T. Taniguchi, and P. Jarillo-Herrero, *Science* **372**, 1458 (2021).